Self-reproducing catalyst drives repeated phospholipid synthesis and membrane growth

Michael D. Hardy[a], Jun Yang[a], Jangir Selimkhanov[b], Christian M. Cole[a], Lev S. Tsimring[b], and Neal K. Devaraj[a,1]

[a]Department of Chemistry and Biochemistry, University of California, San Diego, La Jolla, CA 92093; and [b]The BioCircuits Institute, University of California, San Diego, La Jolla, CA 92093

Edited by Jack W. Szostak, Massachusetts General Hospital, Boston, MA, and approved May 15, 2015 (received for review April 9, 2015)

Cell membranes are dynamic structures found in all living organisms. There have been numerous constructs that model phospholipid membranes. However, unlike natural membranes, these biomimetic systems cannot sustain growth owing to an inability to replenish phospholipid-synthesizing catalysts. Here we report on the design and synthesis of artificial membranes embedded with synthetic, self-reproducing catalysts capable of perpetuating phospholipid bilayer formation. Replacing the complex biochemical pathways used in nature with an autocatalyst that also drives lipid synthesis leads to the continual formation of triazole phospholipids and membrane-bound oligotriazole catalysts from simpler starting materials. In addition to continual phospholipid synthesis and vesicle growth, the synthetic membranes are capable of remodeling their physical composition in response to changes in the environment by preferentially incorporating specific precursors. These results demonstrate that complex membranes capable of indefinite self-synthesis can emerge when supplied with simpler chemical building blocks.

membranes | autocatalysis | self-assembly | lipids

Lipid membranes are ubiquitous in all domains of life. Membranes are organizing structures needed to define physical boundaries, compartmentalize molecules within the cell, and provide sites for proteins that control transport and signaling. Natural membranes are also capable of growth through in situ synthesis of glycerophospholipids catalyzed by embedded integral membrane proteins that are continually synthesized by entrapped cellular machinery (1–3). Numerous studies of artificial membranes have demonstrated the ability of various amphiphiles to self-assemble into bilayer vesicles with properties reminiscent of cellular membranes (4–8). A limited number of these studies have demonstrated that seeding artificial membranes with catalysts that are capable of either generating additional amphiphiles, or of driving the recruitment of lipids from the environment, triggers an increase in membrane surface area, and, in some cases, causes vesicle budding and division (9–14). However, membrane growth in these systems inevitably leads to dilution of the catalyst and cessation of membrane formation (15, 16). Thus, a significant roadblock to synthetic membranes capable of continual phospholipid synthesis has been the lack of a mechanism by which the embedded molecular catalysts that are responsible for membrane expansion are able to repopulate indefinitely (15, 17). Here we report on the design of a simplified lipid synthesizing membrane that uses a synthetic, membrane-embedded catalyst that is capable of self-reproduction. To achieve simultaneous lipid and catalyst synthesis we use a shared catalytic triazole coupling reaction to generate both triazole phospholipids and additional membrane-embedded copper-chelating oligotriazole catalysts (18, 19). By substituting the complex network of biochemical pathways used in nature with a single autocatalyst that simultaneously drives membrane growth, our system continually transforms simpler, high-energy building blocks into new artificial membranes.

Results and Discussion

The formation of triazoles by copper catalyzed azide-alkyne cycloaddition is highly selective, has a high thermodynamic driving force (-52 kcal·mol^{-1}), and often works best in water (20). Several oligotriazole ligands are capable of coordinating to Cu^{1+} and promoting triazole catalysis in the presence of oxygen and metal coordinating buffers (21). Because these ligands are themselves synthesized by triazole formation, autocatalysis is possible. Our oligotriazole catalyst was synthesized by combining a tripropargylamine scaffold with 1-azidododecane, forming a Tris-(lauryl triazole)amine (TLTA) ligand. In the presence of Cu^{1+} ions and buffer, the TLTA trimer serves as a selective catalyst for further TLTA ligand synthesis, completing an autocatalytic cycle (Fig. 1*A*). The choice of long-chain alkyl azide molecules was motivated by two factors. First, the three 12-carbon alkyl chains of TLTA promote its association with the lipid bilayer (*SI Appendix*, Fig. S1), enabling catalytic membranes to synthesize phospholipid in the presence of reactive precursors. Second, alkyl azides also serve as precursors for the formation of triazole phospholipids when combined with alkyne lysophospholipids (Fig. 1*B*) (18). Use of two different alkyne precursors and a shared alkyl azide enables the concurrent formation of TLTA and triazole phospholipid while avoiding unproductive side reactions (Fig. 1*C*). The use of common elements in the precursor pool greatly simplifies this system compared with previously described biomimetic membranes.

When phospholipid vesicles containing TLTA (5 μM) are incubated with a solution containing TLTA precursors and Cu^{1+} ions, self-reproduction of TLTA ligand occurs (vesicles characterized by dynamic light scattering and transmission electron microscopy; *SI Appendix*, Fig. S2). Background reaction is

Significance

We report on the design and synthesis of an artificial cell membrane that sustains continual growth. Lipid membranes are ubiquitous in all domains of life. Numerous studies have exploited the ability of lipids to self-assemble into bilayer vesicles with properties reminiscent of cellular membranes, but previous work has yet to mimic nature's ability to support persistent phospholipid membrane formation. In this work, we have developed an artificial cell membrane that continually synthesizes all of the components needed to form additional catalytic membranes. These results demonstrate that complex lipid membranes capable of indefinite self-synthesis can emerge when supplied with simpler chemical building blocks.

Author contributions: M.D.H., J.S., L.S.T., and N.K.D. designed research; M.D.H., J.Y., J.S., and C.M.C. performed research; J.Y., J.S., and C.M.C. contributed new reagents/analytic tools; M.D.H., J.S., C.M.C., L.S.T., and N.K.D. analyzed data; and M.D.H., J.S., L.S.T., and N.K.D. wrote the paper.

The authors declare no conflict of interest.

This article is a PNAS Direct Submission.

[1]To whom correspondence should be addressed. Email: ndevaraj@ucsd.edu.

This article contains supporting information online at www.pnas.org/lookup/suppl/doi:10.1073/pnas.1506704112/-/DCSupplemental.

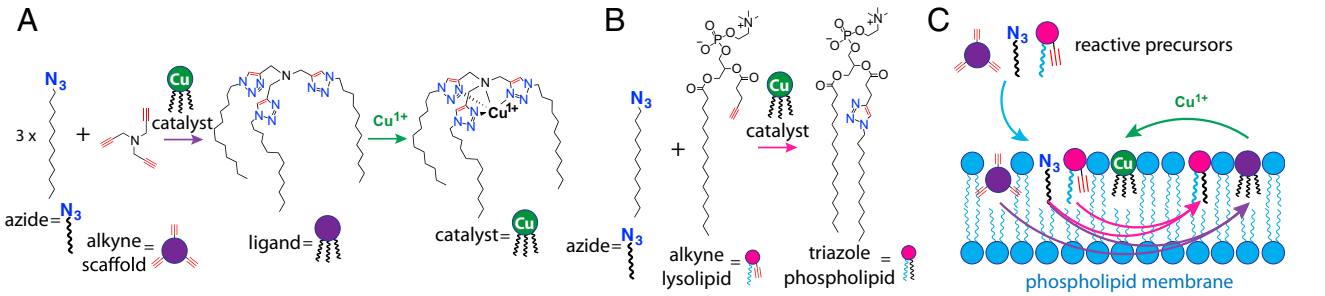

Fig. 1. A self-reproducing catalyst drives triazole phospholipid synthesis and membrane growth. (*A*) The oligotriazole TLTA (ligand) is capable of binding Cu^{1+} ions to form a catalytic complex (catalyst). The copper complex catalyzes the synthesis of new ligand from 1-azidododecane (azide) and tripropargylamine (alkyne scaffold), which, upon metallation, produces additional catalytic molecules. (*B*) The copper complex also catalyzes the formation of triazole phospholipid from 1-azidododecane (azide) and an alkyne modified lysolipid. (*C*) Membrane-embedded catalysts act on azide and alkyne reactive precursors, synthesizing additional phospholipid and oligotriazole ligands, which, upon metallation, become new catalysts. For purposes of illustration, precursors, catalyst ,and triazole phospholipid are only depicted on one leaflet.

inhibited by the presence of N-[Tris(hydroxymethyl)methyl]-2-aminoethanesulfonic acid (TES) buffer (140 mM), a Good's buffer that can weakly coordinate free copper (22). Using liquid chromatography–mass spectrometry–evaporative light scattering detection (LC-MS-ELSD) to monitor ligand synthesis (*SI Appendix*, Figs. S3 and S4), we observe sigmoidal growth curves made up of an induction period, followed by a rapid rise in ligand formation, inflection, and, finally, a plateau as reactants are completely consumed (Fig. 2*A*). Such curves are a hallmark of autocatalytic processes (23, 24), which require time for a buildup of sufficient catalyst, at which point product conversion sharply accelerates. Increasing the amount of initial ligand from 5 μM to 35 μM accelerates the rate of consumption of ligand precursors, with the time required to synthesize 50% of new ligand decreasing from 1.94 h to 0.81 h. The membrane-bound catalyst is also required for the in situ synthesis of triazole phospholipids (Fig. 2*B*). Phospholipid vesicles containing different concentrations of TLTA ligand were incubated with 1-azidododecane and alkyne lysolipid as well as an excess supply of Cu^{1+} ions (120 μM). Vesicle populations possessing higher concentrations of sequestered TLTA ligand synthesize triazole phospholipids more rapidly.

Catalyst reproduction and phospholipid synthesis are both driven by the presence of TLTA. We therefore predicted a synergistic effect between the rate of production of catalytic molecules and the rate of production of membrane building blocks, because TLTA self-reproduction would increase the concentration of catalyst and, in turn, increase the rate of triazole phospholipid synthesis. To test these effects, we incubated vesicles containing TLTA with lipid precursors and measured the amount of triazole phospholipid synthesis in the presence and absence of the essential catalyst precursor tripropargylamine (Fig. 2*C* and *SI Appendix*, Fig. S5). In the absence of tripropargylamine, the catalyst concentration stays constant and the phospholipid conversion proceeds slowly over 24 h with partial conversion. However, addition of 50 μM tripropargylamine leads to assembly of additional TLTA (*SI Appendix*, Fig. S5*D*), resulting in faster lipid synthesis (485 μM vs. 150 μM triazole phospholipid synthesized after 24 h).

To gain greater quantitative insight into the kinetics of the combined autocatalytic vesicle membrane growth, we developed a computational model that includes catalyst formation and triazole phospholipid synthesis (*SI Appendix*). Results from this model exhibit the salient features of the self-reproduction process. Furthermore, taking the values of chemical concentrations used in the experiments, we were able to predict the values of kinetic parameters that yielded quantitative agreement between the experimental and modeling results (solid lines, Fig. 2).

Lipid membranes have been shown to promote the reaction of hydrophobic precursors by either acting as a phase-transfer catalyst or through colocalization (6, 9). Although Cu-TLTA is a molecular catalyst for azide-alkyne cycloadditions and is required for the synthesis of triazoles, it was unclear whether the presence of phospholipid membranes provides a structured environment that contributes to the rate of the coupling reactions. To test this possibility, we incubated TLTA ligands along with azide and alkyne precursors in the presence and absence of phospholipid membranes (1-palmitoyl-2-oleoyl-*sn*-glycero-3-phosphocholine, POPC) (*SI Appendix*, Fig. S6). We found that TLTA-catalyzed triazole phospholipid synthesis requires the presence of phospholipid membranes. TLTA molecules form an extremely hydrophobic solid at room temperature and are unlikely to be catalytically active in a purely aqueous system without a hydrophobic component. Phospholipid membranes are capable of solubilizing the ligand (as indicated by LC-MS) as well as the precursors and intermediates that are needed for TLTA self-synthesis.

We next determined the effect of phospholipid concentration on autocatalyst synthesis (*SI Appendix*, Fig. S7). Interestingly, the synthesis of new autocatalyst is directly dependent upon the amount of lipid present. This may be attributed to increased partitioning of precursors, intermediates, and products into the lipid phase (25, 26), indicating that, at these concentrations, phase transfer catalysis or colocalization effects outweigh possible dilution of the reactants in additional membrane. These results provide further evidence that the presence of membranes confers advantages to the autocatalytic reactions and establishes a synergistic relationship between autocatalysis and phospholipid synthesis.

Membrane growth in the presence of lipid precursors is an important attribute of living cellular membranes. Synthetic vesicles containing TLTA are capable of synthesizing both molecular catalysts and phospholipids when exposed to appropriate catalyst and phospholipid azide and alkyne precursors (Fig. 2*C* and *SI Appendix*, Figs. S3–S6). To determine whether the synthetic vesicles can continually catalyze lipid synthesis (Fig. 3*A*), vesicles containing 0 or 10 mol% TLTA were added to a precursor solution containing tripropargylamine, alkyne lysolipid, 1-azidododecane, and Cu^{1+} ions in TES buffer, and synthesis was tracked using LC-MS-ELSD (Fig. 3*B* and *SI Appendix*, Fig. S8). Vesicles without TLTA (negative control) were unable to synthesize TLTA or triazole phospholipid (*SI Appendix*, Fig. S8). Vesicles with TLTA converted reactive precursors to membrane-bound vesicles consisting of triazole phospholipid and TLTA. To create additional synthetic membranes after the precursors had been consumed, we combined 10% of the formed vesicle solution with a new solution containing both lipid and catalyst precursors. Again, TLTA vesicles converted the substrate solution into vesicles consisting of triazole phospholipid and TLTA. When the negative control was similarly transferred to a new

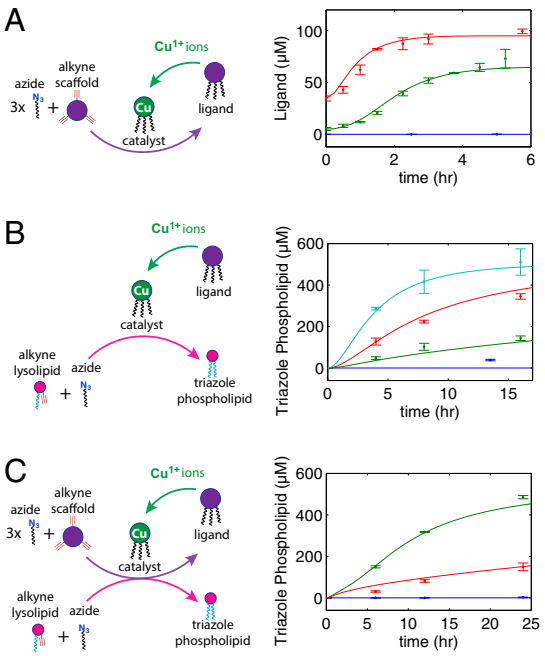

Fig. 2. Monitoring of catalytic ligand and lipid synthesis in preformed membranes. (*A*) Autocatalytic synthesis of TLTA ligands in vesicle membranes loaded with 0 (blue), 5 (green), or 35 (red) μM TLTA. (*B*) Triazole phospholipid synthesis using vesicles loaded with 0 (blue), 15 (green), 40 (red), and 100 (cyan) μM TLTA. (*C*) The rate of triazole phospholipid synthesis in the presence of vesicles loaded with 75 μM TLTA is significantly higher in the presence of the ligand precursor, tripropargylamine (50 μM) (green), and sluggish in its absence (red), owing to an inability to form additional Cu-TLTA catalyst (*SI Appendix*, Fig. S5). No triazole phospholipid is synthesized without the presence of the TLTA ligand (blue). Model-generated fits (solid lines) agree well with the experimental data. The concentration of copper is 120 μM, and the concentration of TES is 140 mM for *A* and *B* and 350 mM for *C*. Concentrations were determined by fitting absorbance data from HPLC to a calibration curve. Full equations and fitted parameter values are available in *SI Appendix*. Error bars represent SDs ($n = 3$).

solution, no new substrate was converted to vesicles. Additionally, each transfer resulted in a 90% reduction in POPC (*SI Appendix*, Fig. S8). Upon propagating synthetic membranes into a new solution for a second time, the initial seed concentration of POPC was reduced from 200 μM to 2 μM, and no phospholipid was detected in the negative control after two transfers (*SI Appendix*, Fig. S8). Under optimized conditions, we typically achieved 95% conversion of the lipid precursors over a period of 20–35 h. We repeated this process 15 times over a period of 500 h, showing that it seems to be repeatable indefinitely in the presence of simpler precursors that permit the synthesis of both the catalysts and their membrane product (*SI Appendix*, Fig. S9).

We next monitored the growth of vesicles using time-lapse fluorescence microscopy and an automatic vesicle tracking algorithm based on a previously developed, single-cell tracking algorithm that monitors vesicle size and location (27). When catalytic membranes from a serial transfer experiment, as in Fig. 3*A*, were added to solutions containing reactive precursors and 0.1 mol% membrane staining dye (Rh-DHPE), spherical structures appeared that increased slowly in size over a period of hours (Fig. 4*A* and *SI Appendix*, Fig. S10). In all imaging experiments, vesicles identified with fluorescence were distinguished from possible azide oil-related artifacts by bright-field microscopy (*SI Appendix*, Fig. S11), which highlights a significant refractive difference between aqueous vesicle compartments and oil emulsions (1.33 vs. 1.42) (28). Some of these vesicles grew from <1 μm to upwards of 5 μm in diameter (Fig. 4*B*). In addition, we find that the majority of membranes grow from sizes undetectable by fluorescent microscopy to a wide range of smaller-sized vesicles (1–2 μm), significantly increasing total membrane area (Fig. 4*C*). Vesicles incapable of synthesizing triazole phospholipid (lacking copper or TLTA) did not undergo growth (*SI Appendix*, Fig. S12), ruling out the possibility that vesicle growth was due to phospholipid spreading out on the glass slide, interactions of vesicles with alkyl azide oil droplets, or vesicle fusion.

Previous work has demonstrated that vesicles undergo shape transformations when the acquisition of new lipids is fast and solute permeation across membranes is slow (29), and this could account for a number of structures observed here (Fig. 4*D*, *SI Appendix*, Figs. S13 and S17, and Movie S1). We infer that the flux of osmolytes across lipid bilayers and the rate of lipid synthesis are sufficiently compatible to prevent vesicle collapse and allow for an increase in both vesicle volume and membrane surface area. Swelling of vesicle volume suggests a net positive flux of solutes into the vesicle interior. Model systems of phospholipid vesicles indicate that membranes are permeable to protons, ions, and small charged molecules (30–33). Chakrabarti and Deamer (30) found that even zwitterionic amino acids, such as serine, could equilibrate across a phospholipid bilayer in as short a time as 2 h under certain conditions. The lack of a strong pH effect on the permeability coefficients of measured charged species supports a transient defect mechanism of membrane permeation over a solubility-diffusion mechanism (32). Transient defects are postulated to increase in bilayers when imbedded structures, such as proteins, are present or when bilayers are osmotically stressed (31, 34–36), and it is therefore possible that Cu-TLTA, precursors, and TLTA intermediates could increase the incidence of transient defects.

To quantify vesicle growth, we fluorescently labeled and imaged vesicles from a serial transfer experiment before and after reaction with excess precursors. Larger, readily visible vesicles were counted across 100 frame captures, and it was found that the number of large (>100 pixels) vesicles increased by approximately threefold after reaction with reactive precursors (*SI Appendix*, Fig. S14). The increase in the number of large objects might suggest that the synthetic membranes have mechanisms for reproduction during their growth phase, but it might

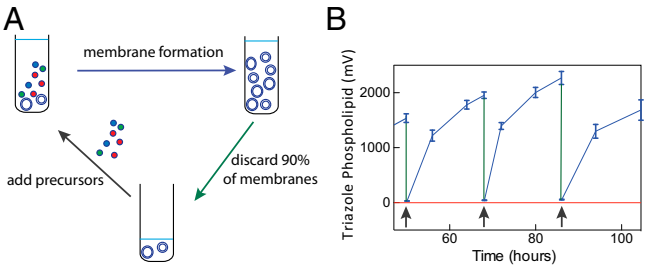

Fig. 3. Continual synthesis of catalytic membranes through serial transfers. (*A*) Vesicles containing embedded ligands are combined with a solution containing ligand and phospholipid precursors, as well as a source of Cu^{1+} (black arrow). Over time, these precursors are converted to additional catalytic vesicles (blue arrow). Once the precursors are depleted, a fraction (10%) of the vesicle population is isolated (green arrow) and combined with a fresh precursor solution, enabling further membrane formation. (*B*) Triazole phospholipid vesicle synthesis with sequential serial transfers of vesicles containing TLTA ligands (blue line) into fresh precursor solutions shows repeated and long-term (>500 h, *SI Appendix*, Fig. S9) phospholipid formation relative to control vesicles lacking TLTA ligands (red line). Black arrows indicate the time at which vesicle transfer to new precursor solutions took place. Phospholipid was monitored using LC-MS-ELSD measurements (raw ELSD data shown). Initial conditions for displayed rounds: 120 μM $CuSO_4$, 60 μM hydroquinone, 450 mM TES, 40 mM Mops, 54 μM tripropargylamine, 558 μM alkyne lysolipid, and 925 μM alkyl azide. Error bars represent SDs ($n = 3$).

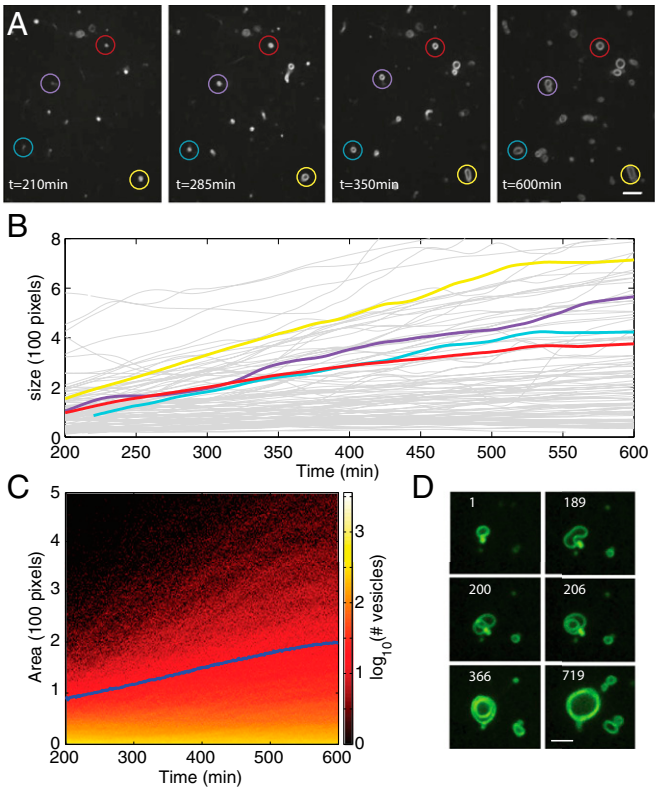

Fig. 4. Monitoring growth of vesicles composed of catalytic membranes. Initial conditions: 132 μM $CuSO_4$, 60 μM hydroquinone, 450 mM TES, 40 mM Mops, 60 μM tripropargylamine, 558 μM alkyne lysolipid, and 925 μM alkyl azide. (*A*) Larger vesicles emerge from the growth of smaller catalytic vesicles exposed to ligand and lipid precursors. Vesicle growth could be monitored using a membrane-staining fluorescent dye (Rh-DHPE) and time-lapse confocal microscopy. Vesicles grew in size over several hours and their size and location were tracked using an automatic vesicle tracking algorithm based on a previously developed single-cell tracking algorithm (25). (Scale bar, 5 μm.) (*B*) Multiple single vesicle area trajectories show growth over a period of 400 min. Highlighted color trajectories correspond to the vesicles within corresponding colored circles in *A*. (*C*) The total fluorescent area (blue curve) corresponding to total membrane formed increased significantly during the experiment, before leveling off. The heat map shows the number of vesicles having a given size (measured in number of pixels) at a given time point. The map shows an increase in number of vesicles as well as the size of those vesicles over time. (*D*) Lipid synthesis-mediated growth results in an increase in membrane surface area and volume. Previous work has demonstrated that vesicle shape transformations can arise when membrane surface area increases more rapidly than vesicle volume (29). The shape change depicted here results in the formation of a multilameller vesicle at 206 min. Numbers indicate elapsed time, in minutes, from start of imaging. (Scale bar, 3 μm.)

also suggest that large vesicles are simply emerging from the growth of smaller vesicles initially imperceptible with microscopy.

We next set out to elucidate the mechanism by which vesicles increase in number when an excess of precursors are present. One possible route could mirror bacterial cell division: A cell increases both internal volume and membrane surface area before budding, pinching off, and dividing into two cells. Alternatively, new catalytic vesicles could be synthesized de novo at the outer leaflet of preexisting catalytic vesicles. This route might catalyze new triazole lipid and autocatalyst without transferring either preexisting membrane or encapsulated contents to new vesicles, so we refer to this pathway as vesicle nucleation, and not division. Because vesicle contents would not be transferred from seed vesicles to new vesicles in this process, the use of a membrane-impermeable water-soluble dye [hydroxyl pyrene trisulfonic acid (HPTS)] could be used to distinguish division from nucleation.

Both vesicle division and nucleation might be unobservable or difficult to distinguish with light microscopy if the diameters of new vesicles are smaller than 250 nm. To address these challenges, we desired a well-defined initial population of vesicles large enough to be readily observable with light microscopy. Large multilamellar vesicles (MLVs) bearing catalysts and encapsulating HPTS were prepared by adapting a previously established procedure (37). MLVs were observed throughout the duration of experiments (up to 60 h), indicating that vesicles are stable in the presence of alkyne lysolipid and alkyl azide and retain their contents over time (Fig. 5). We observed the formation of numerous additional vesicles when TLTA-bearing MLVs were incubated with azide and alkyne reactants and exposed to copper. A negative control was also performed, which differed only in that the identical MLVs were not exposed to copper (Fig. 5 *A* and *B*). To quantify this result, we counted 20 contiguous tiles, like those shown in Fig. 5 *A* and *B*, from the MLV samples containing or lacking copper. Three replicates were performed and results were averaged together. The TLTA vesicle population exposed to copper had an approximate four-fold increase in the number of vesicles compared with the same initial TLTA vesicle population from which copper was excluded (Fig. 5*C*). LC-MS-ELSD data provide further support for additional membrane formation by demonstrating that triazole phospholipid and additional TLTA is synthesized when copper is present, whereas neither product is synthesized in the absence of copper (*SI Appendix*, Fig. S15).

Having results suggesting a mechanism of division that transfers encapsulated contents from parent to daughter vesicles, we next used spinning disk confocal microscopy to capture division processes in situ. HPTS vesicles were immersed with precursors and loaded onto a slide, and MLV tomography was performed. Computed tomograms of MLVs and the surrounding space were constructed with Imaris 7.6 software (Fig. 6). Capturing the space surrounding MLVs was essential to exclude the possibility that observed daughter vesicles were merely preexisting vesicles that had diffused into the frame. Representative vesicle division events from a single MLV are highlighted in Fig. 6. Division events were not observed with negative controls lacking copper (*SI Appendix*, Fig. S16). Additional data suggest that some division events are preceded by the growth, collapse, and reorganization of tubule structures (*SI Appendix*, Fig. S17). Division events were not observed in control experiments lacking copper. Based on previous studies, we speculate that the observed vesicle morphological changes can be explained by in situ phospholipid synthesis, which drives an increase in the vesicle surface area-to-volume ratio (29, 38–42). To compensate for the increased membrane material and relieve curvature stress, the

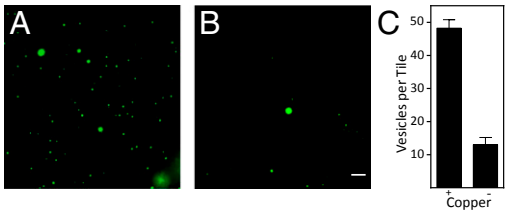

Fig. 5. Triazole phospholipid synthesis leads to an increase in the number of vesicles containing encapsulated contents. Catalytic MLVs containing 10 mol% TLTA and HPTS were added to a solution containing 60 μM hydroquinone, 350 mM TES, 60 μM tripropargylamine, 615 μM alkyne lysolipid, and 1.01 mM alkyl azide. The solution was split into two parts, and 120 μM copper sulfate was added to one (*A*). To the second reaction (*B*), an equivalent volume of water was added in place of copper. (Scale bar, 5 μm.) Vesicles from a matrix of 20 contiguous images were counted on three separate occasions and averaged together (*C*). Error bars represent SDs ($n = 3$).

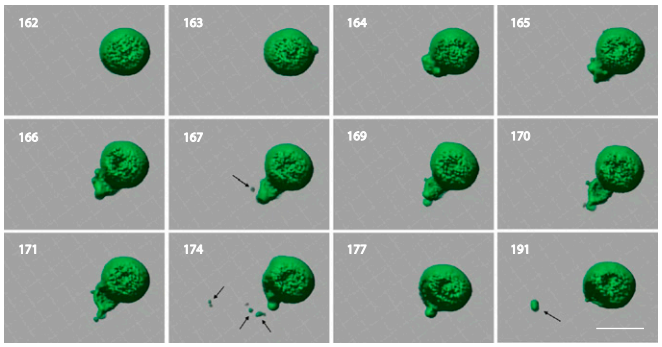

Fig. 6. Monitoring vesicle formation. MLVs with encapsulated HPTS were incubated in 120 μM $CuSO_4$, 60 μM hydroquinone, 350 mM TES, 60 μM tripropargylamine, 615 μM alkyne lysolipid, and 1.01 mM alkyl azide. Small daughter vesicles are highlighted with arrows. Numbers indicate elapsed time, in minutes, from start of experiment. (Scale bar, 5 μm.)

vesicles either adopt nonspherical shapes or spontaneously divide. Additionally, studies indicate vesicles may divide in the presence of externally applied forces (5, 29, 43). Because the vesicles are typically agitated during lipid synthesis, we cannot rule out that mechanical stress during lipid synthesis also contributes to new vesicle formation.

Having observed evidence for vesicle division, we next set out to test whether catalytic vesicles seed the nucleation of new vesicles. Texas Red-DHPE was added to large HPTS-encapsulating catalytic MLVs in the presence of precursors. Sonicated vesicles were also prepared with HPTS and used for experiments, and unencapsulated dye was separated from vesicles by 10 rounds of dialysis with spin filters. We found that Texas Red-DHPE–labeled vesicles lacking HPTS emerge adjacent to preformed catalytic vesicles and grow larger with time (*SI Appendix*, Fig. S18), recapitulating previous observations of observed growth. These results strongly suggest the presence of a vesicle nucleation pathway that does not transfer encapsulated contents from preexisting vesicles to new vesicles.

Catalytic membranes may have preceded the origin of life, and computational models have predicted that prebiotic systems lacking nucleic acids might be able to propagate compositional information and be capable of adaptation (44). To test whether the catalytic membranes preferentially incorporate specific precursors, we incubated TLTA-containing bilayers with an equal mixture of 1-azidodecane and 1-azidohexadecane. Assuming random uptake, one would expect an equal amount of triazole phospholipid incorporating 12-carbon and 16-carbon alkyl chains as well as four different oligotriazole ligands with a 1:3:3:1 distribution. Instead, there was a significant enrichment of the 16-carbon chain, both in the phospholipid and in the autocatalyst (Fig. 7). This result may be due to the predicted increased retention time of the 16-carbon azide in the reactive membranes compared with the 12-carbon azide, increasing the likelihood of interaction with the membrane-bound catalyst and alkyne lysolipid (45, 46). We also tested whether the selectivity of 1-azidohexadecane incorporation can be modulated by changing the environment. Because coordinating salts impede the reaction, we compared vesicles incubated at two different concentrations of TES buffer. Significantly greater relative selection for 1-azidohexadecane vs. 1-azidododecane in both the phospholipid and oligotriazole is observed at an elevated coordinating buffer concentration (Fig. 7). The diminished synthesis rate seems to further bias reaction preference toward the 16-carbon azide precursors, which are retained longer in the membranes.

Although this abiotic system is exceedingly simplified in comparison, the described catalytic membranes bear several similarities to native cellular membranes. Sequestration of the TLTA catalyst in the membrane mimics the location of the membrane-bound enzymes that typically catalyze lipid synthesis (1, 2) and enables catalysts and organic precursors to achieve high local concentrations, avoid problems with membrane permeability as a barrier to substrate diffusion, and prevent loss of material during vesicle division. Additionally, the observed growth driven by lipid synthesis resembles a form of biological membrane growth that can be carried out by minimal living organisms. For instance, recent studies have shown that L-form bacteria that lack cell walls and division machinery undergo membrane growth and division when lipid synthesis is allowed to continue (47–49). Finally, the finding that catalytic membranes can undergo dynamic changes in physical composition in response to changes in environmental conditions resembles the well-known ability of living cell membranes to rapidly adapt their lipid membrane structure in response to external stimuli (50, 51). Membranes that preceded life may have also behaved similarly, and computational models posit that catalytic assemblies can exhibit a fair degree of homeostasis and can be thought of as primitive "compositional genomes" (44).

We have designed a self-reproducing coupling catalyst that can drive the repeated synthesis of synthetic phospholipid membranes. Unlike previous work with synthetic membranes that couples bilayer growth to the breakdown of reactive lipid precursors (6, 10), this system uses simpler reactive starting materials to build up both functionally complex phospholipids and the catalysts that drive their synthesis. The formation of robust phospholipid-like membrane constituents ensures membrane stability, even in high concentrations of a biocompatible Good's buffer such as TES or in the presence of divalent metal ions. This stability in the presence of conditions that also permit naturally occurring biochemical reactions to take place will likely facilitate interfacing of synthetic membrane-bound vesicles with biological materials (e.g., oligonucleotides and cell-free translation systems). Furthermore, lipid-synthesizing catalysts likely conferred a selective advantage upon early protocells (52), and although no organisms are thought to use the copper-catalyzed cycloaddition reaction, integrating Cu-TLTA self-reproducing catalysts with model systems of fatty acid membranes may enable future studies exploring the role of phospholipid-synthesizing catalysts in the competitive growth and division of protocells (52).

Methods

Chemical Synthesis. Full experimental details that describe the synthesis and characterization of all compounds can be found in *SI Appendix*, *Supplementary Materials*.

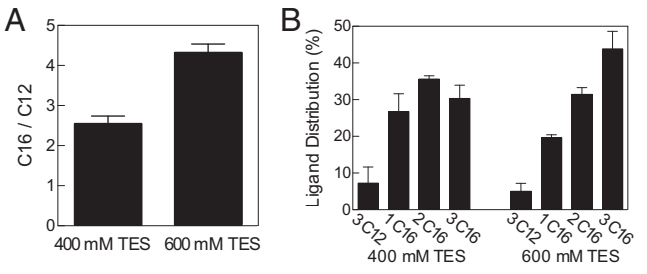

Fig. 7. Preferential incorporation of reactive precursors. (*A*) Catalytic membranes formed from a 12-carbon alkyl azide were combined with a precursor solution, containing 1.86 mM of a 1:1 mixture of 12-carbon and 16-carbon alkyl azides, and showed preferential incorporation of 16-carbon azides. The ratio of triazole phospholipid formed from 1-azidohexadecane (C16) vs. 1-azidododecane (C12) is greater in the presence of a higher concentration of coordinating buffer. (*B*) The relative distribution of the various triazole ligands, formed from C12 and C16 mixtures at 400 mM (left) and 600 mM (right) coordinating buffer concentration, shows increased incorporation of C16 at higher TES concentration. Error bars represent SD ($n = 3$).

Vesicle Preparation. POPC in chloroform and TLTA in chloroform were added to a glass vial, placed under nitrogen, and dried to prepare a lipid film. Dried films were hydrated in a buffer containing 40 mM Mops and 140 mM to 600 mM TES (pH 8.45–8.5). Solutions were briefly vortexed and then sonicated for 85 min (final temperature 56–62 °C). Vesicle preparations were cooled to room temperature, transferred to Eppendorf tubes, and sonicated for 20–25 additional minutes without heat.

Preparation of Reactive Precursors. Emulsions of alkyl azide and alkyne lysolipid were prepared by adding 21.6 μL of 30 mM alkyl azide in chloroform and 13 μL of 15 mM alkyne lysolipid in chloroform to a glass vial and drying off the chloroform with filtered nitrogen. A buffer with 40 mM Mops and a TES concentration, matching the vesicle population to be used for the experiment, was then added, creating emulsions. The solution was briefly vortexed and sonicated without heat for 15–30 min.

Cu-Ligand Catalyzed Cycloaddition Reactions. $CuSO_4$ (8 mM) and hydroquinone (4 mM) were prepared daily with H_2O obtained from a Milli·Q Water Purification System. Tripropargylamine (5 mM, unless stated otherwise) was prepared in 100% EtOH. All reactions were performed in 2 mL Eppendorf tubes, which sat on a shaker, rotating ~120 revolutions per minute at room temperature. Concentrations reported were based on a calibration curve created using known concentrations of the respective compound.

LC/MS/ELSD. All experiments were monitored using an Agilent 1260 Infinity Series HPLC with an Agilent Zorbax eclipse plus C8 column, a 380 Varian-Agilent ELSD, and a 6100 Agilent Quadrupole MS. For all experiments, 15-μL aliquots sampled directly from reactions were loaded into the LCMS for 10-μL injections.

Microscopy. Microscopy of a serial transfer experiment was performed following the addition of $CuSO_4$ to each reaction mixture. Ten microliters of reaction mixture was placed on a glass slide and covered with a no. 1 coverslip, which was subsequently sealed with nail polish to prevent dehydration.

ACKNOWLEDGMENTS. The authors acknowledge helpful discussions with Prof. Christopher Wills, Dr. Itay Budin, Prof. Simpson Joseph, Prof. Russell Doolittle, and Prof. James Collman. This material is based upon work supported in part by the University of California, San Diego; the US Army Research Laboratory; the US Army Research Office under Grant W911NF-13-1-0383; and National Science Foundation Grant CHE-1254611. L.S.T. acknowledges partial support from NIH Grant P50GM085764. M.D.H. acknowledges support from NIH Training Grant T32 GM007240.

1. Shindou H, Hishikawa D, Harayama T, Yuki K, Shimizu T (2009) Recent progress on acyl CoA:lysophospholipid acyltransferase research. *J Lipid Res* 50(Suppl):S46–S51.
2. Shindou H, Shimizu T (2009) Acyl-CoA:lysophospholipid acyltransferases. *J Biol Chem* 284(1):1–5.
3. Zhang YM, Rock CO (2008) Thematic review series: Glycerolipids. Acyltransferases in bacterial glycerophospholipid synthesis. *J Lipid Res* 49(9):1867–1874.
4. Chen IA, Roberts RW, Szostak JW (2004) The emergence of competition between model protocells. *Science* 305(5689):1474–1476.
5. Hanczyc MM, Fujikawa SM, Szostak JW (2003) Experimental models of primitive cellular compartments: Encapsulation, growth, and division. *Science* 302(5645):618–622.
6. Wick R, Walde P, Luisi PL (1995) Light-microscopic investigations of the autocatalytic self-reproduction of giant vesicles. *J Am Chem Soc* 117(4):1435–1436.
7. Hargreaves WR, Deamer DW (1978) Liposomes from ionic, single-chain amphiphiles. *Biochemistry* 17(18):3759–3768.
8. Brea RJ, Cole CM, Devaraj NK (2014) In situ vesicle formation by native chemical ligation. *Angew Chem Int Ed Engl* 53(51):14102–14105.
9. Adamala K, Szostak JW (2013) Competition between model protocells driven by an encapsulated catalyst. *Nat Chem* 5(6):495–501.
10. Kurihara K, et al. (2011) Self-reproduction of supramolecular giant vesicles combined with the amplification of encapsulated DNA. *Nat Chem* 3(10):775–781.
11. Takakura K, Toyota T, Sugawara T (2003) A novel system of self-reproducing giant vesicles. *J Am Chem Soc* 125(27):8134–8140.
12. Wick R, Luisi PL (1996) Enzyme-containing liposomes can endogenously produce membrane-constituting lipids. *Chem Biol* 3(4):277–285.
13. Deamer DW, Boatman DE (1980) An enzymatically driven membrane reconstitution from solubilized components. *J Cell Biol* 84(2):461–467.
14. Suzuki K, Toyota T, Takakura K, Sugawara T (2009) Sparkling morphological changes and spontaneous movements of self-assemblies in water induced by chemical reactions. *Chem Lett* 38(11):1010–1015.
15. Stano P, Luisi PL (2010) Achievements and open questions in the self-reproduction of vesicles and synthetic minimal cells. *Chem Commun (Camb)* 46(21):3639–3653.
16. Deamer D (2005) A giant step towards artificial life? *Trends Biotechnol* 23(7):336–338.
17. Kamioka S, Ajami D, Rebek J, Jr (2010) Autocatalysis and organocatalysis with synthetic structures. *Proc Natl Acad Sci USA* 107(2):541–544.
18. Budin I, Devaraj NK (2012) Membrane assembly driven by a biomimetic coupling reaction. *J Am Chem Soc* 134(2):751–753.
19. Rostovtsev VV, Green LG, Fokin VV, Sharpless KB (2002) A stepwise huisgen cycloaddition process: Copper(I)-catalyzed regioselective "ligation" of azides and terminal alkynes. *Angew Chem Int Ed Engl* 41(14):2596–2599.
20. Meldal M, Tornøe CW (2008) Cu-catalyzed azide-alkyne cycloaddition. *Chem Rev* 108(8):2952–3015.
21. Chan TR, Hilgraf R, Sharpless KB, Fokin VV (2004) Polytriazoles as copper(I)-stabilizing ligands in catalysis. *Org Lett* 6(17):2853–2855.
22. Good NE, et al. (1966) Hydrogen ion buffers for biological research. *Biochemistry* 5(2):467–477.
23. Robertson A, Sinclair AJ, Philp D (2000) Minimal self-replicating systems. *Chem Soc Rev* 29(2):141–152.
24. Jackson WG, Freasier B, Goodyear K, Cooper JN (2003) Sulfite ion substitution of trans-dichlorobis(ethylenediamine)cobalt(III): A classic autocatalytic reaction. *Inorg Chim Acta* 355:137–143.
25. Walde P, Wick R, Fresta M, Mangone A, Luisi PL (1994) Autopoietic self-reproduction of fatty-acid vesicles. *J Am Chem Soc* 116(26):11649–11654.
26. Bunton CA, Robinson L (1968) Micellar effects upon nucleophilic aromatic and aliphatic substitution. *J Am Chem Soc* 90(22):5972–5979.
27. Mondragón-Palomino O, Danino T, Selimkhanov J, Tsimring L, Hasty J (2011) Entrainment of a population of synthetic genetic oscillators. *Science* 333(6047):1315–1319.
28. Dornte RW, Smyth CP (1930) The dielectric polarization of liquids X The polarization and refraction of the normal paraffins. *J Am Chem Soc* 52:3546–3552.
29. Zhu TF, Szostak JW (2009) Coupled growth and division of model protocell membranes. *J Am Chem Soc* 131(15):5705–5713.
30. Chakrabarti AC, Deamer DW (1992) Permeability of lipid bilayers to amino acids and phosphate. *Biochim Biophys Acta* 1111(2):171–177.
31. Deamer DW, Nichols JW (1983) Proton-hydroxide permeability of liposomes. *Proc Natl Acad Sci USA* 80(1):165–168.
32. Paula S, Volkov AG, Van Hoek AN, Haines TH, Deamer DW (1996) Permeation of protons, potassium ions, and small polar molecules through phospholipid bilayers as a function of membrane thickness. *Biophys J* 70(1):339–348.
33. Nagle JF, Scott HL, Jr (1978) Lateral compressibility of lipid mono- and bilayers. Theory of membrane permeability. *Biochim Biophys Acta* 513(2):236–243.
34. Oglęcka K, Rangamani P, Liedberg B, Kraut RS, Parikh AN (2014) Oscillatory phase separation in giant lipid vesicles induced by transmembrane osmotic differentials. *eLife* 3:e03695.
35. Sandre O, Moreaux L, Brochard-Wyart F (1999) Dynamics of transient pores in stretched vesicles. *Proc Natl Acad Sci USA* 96(19):10591–10596.
36. Engel MF, et al. (2008) Membrane damage by human islet amyloid polypeptide through fibril growth at the membrane. *Proc Natl Acad Sci USA* 105(16):6033–6038.
37. Zhu TF, Szostak JW (2009) Preparation of large monodisperse vesicles. *PLoS ONE* 4(4):e5009.
38. Berclaz N, Muller M, Walde P, Luisi PL (2001) Growth and transformation of vesicles studied by ferritin labeling and cryotransmission electron microscopy. *J Phys Chem B* 105(5):1056–1064.
39. Peterlin P, Arrigler V, Kogej K, Svetina S, Walde P (2009) Growth and shape transformations of giant phospholipid vesicles upon interaction with an aqueous oleic acid suspension. *Chem Phys Lipids* 159(2):67–76.
40. Svetina S (2009) Vesicle budding and the origin of cellular life. *ChemPhysChem* 10(16):2769–2776.
41. Bozic B, Svetina S (2004) A relationship between membrane properties forms the basis of a selectivity mechanism for vesicle self-reproduction. *Eur Biophys J* 33(7):565–571.
42. Terasawa H, Nishimura K, Suzuki H, Matsuura T, Yomo T (2012) Coupling of the fusion and budding of giant phospholipid vesicles containing macromolecules. *Proc Natl Acad Sci USA* 109(16):5942–5947.
43. Hanczyc MM, Szostak JW (2004) Replicating vesicles as models of primitive cell growth and division. *Curr Opin Chem Biol* 8(6):660–664.
44. Segré D, Ben-Eli D, Lancet D (2000) Compositional genomes: Prebiotic information transfer in mutually catalytic noncovalent assemblies. *Proc Natl Acad Sci USA* 97(8):4112–4117.
45. Zhang F, Kamp F, Hamilton JA (1996) Dissociation of long and very long chain fatty acids from phospholipid bilayers. *Biochemistry* 35(50):16055–16060.
46. Bird DA, Laposata M, Hamilton JA (1996) Binding of ethyl oleate to low density lipoprotein, phospholipid vesicles, and albumin: A 13C NMR study. *J Lipid Res* 37(7):1449–1458.
47. Leaver M, Domínguez-Cuevas P, Coxhead JM, Daniel RA, Errington J (2009) Life without a wall or division machine in Bacillus subtilis. *Nature* 457(7231):849–853.
48. Mercier R, Kawai Y, Errington J (2013) Excess membrane synthesis drives a primitive mode of cell proliferation. *Cell* 152(5):997–1007.
49. Mercier R, Domínguez-Cuevas P, Errington J (2012) Crucial role for membrane fluidity in proliferation of primitive cells. *Cell Reports* 1(5):417–423.
50. Sinensky M (1974) Homeoviscous adaptation—a homeostatic process that regulates the viscosity of membrane lipids in Escherichia coli. *Proc Natl Acad Sci USA* 71(2):522–525.
51. Ingram LO (1976) Adaptation of membrane lipids to alcohols. *J Bacteriol* 125(2):670–678.
52. Budin I, Szostak JW (2011) Physical effects underlying the transition from primitive to modern cell membranes. *Proc Natl Acad Sci USA* 108(13):5249–5254.